Dipyrromethene as a Ligand for the Stabilization of Low-Valent Gallium Complexes

Tim Richter, Stefan Thum, Timothy Vilpas, Oliver P. E. Townrow, Lukas Klerner, Jens Langer, and Sjoerd Harder*

ABSTRACT: We investigated the low-valent chemistry of Al and Ga with the ligand $^{t\mathrm{Bu}}$DPM, a dipyrromethene ligand scaffold with two large *t*Bu groups in the flanking 1- and 9-positions and a mesityl group in the backbone 5-position. Attempted synthesis of ($^{t\mathrm{Bu}}$DPM)Al$^{\mathrm{I}}$ by reduction of ($^{t\mathrm{Bu}}$DPM)AlI$_2$ with KC$_8$ failed. However, reduction of ($^{t\mathrm{Bu}}$DPM)GaI$_2$ (**1**) with K/KI led to successful isolation of ($^{t\mathrm{Bu}}$DPM)Ga$^{\mathrm{I}}$ (**3**). The Ga$^{\mathrm{II}}$ intermediate in the reduction process crystallized as a digallane: [($^{t\mathrm{Bu}}$DPM)GaI]$_2$ (**2**). Also, **3** crystallized as a dinuclear complex with a Ga−Ga bond. However, in a benzene solution, the **3** dissociates into two mononuclear complexes. Reaction of a benzene solution of ($^{t\mathrm{Bu}}$DPM)Ga$^{\mathrm{I}}$ with excess Me$_3$SiN$_3$ gave the tetrazagallole product ($^{t\mathrm{Bu}}$DPM)Ga[N$_4$(SiMe$_3$)$_2$] (**4**) and not the alternative azide-amide product ($^{t\mathrm{Bu}}$DPM)Ga(N$_3$)[N(SiMe$_3$)$_2$], which according to calculations is thermodynamically considerably more stable. Theoretical investigations on the nature of the Ga−Ga bonds in **2** and **3** and the mechanism for selective formation of **4** have been included.

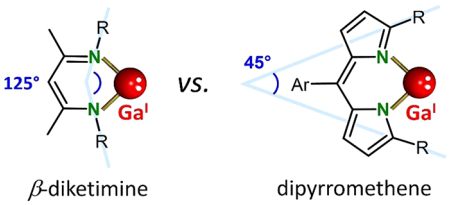

INTRODUCTION

The first organometallic Ga$^{\mathrm{I}}$ compound was reported by Uhl and co-workers in the form of a tetrameric cluster (**I**, Scheme 1).[1] The isolation of monomeric Ga$^{\mathrm{I}}$ complexes typically requires the use of extremely bulky monodentate ligands (**II**)[2] or the use of large multidentate ligands (**III**-**V**).[3−5] Especially the *β*-diketiminate (BDI) ligand (**VI**) has been popular in studying the chemistry of mononuclear, low-valent Ga$^{\mathrm{I}}$ complexes.[6]

A ligand class that shows great similarities to the BDI ligand is based on dipyrromethene (DPM). This unit is a porphyrin substructure which was discovered in 1924 by Fischer and Schubert as part of their investigations on the cleavage products of blood dyes.[7] Its anionic derivatives are frequently used ligand systems that are ubiquitous in boron chemistry. The larger family of highly colorful and fluorescent (DPM)BF$_2$ complexes, also known as BODIPYs, received particular interest in applications as labeling reagents, fluorescent switches, chemosensors and laser dyes.[8] As a monoanionic *N*,*N*-chelating ligand (**VII**), it has also found application in organometallic chemistry, especially as an alternative for the ubiquitously used *β*-diketiminate (BDI) ligands (**VI**).

Although there are certain similarities between BDI and DPM ligands, both are monoanionic *N*,*N*-chelating ligands which can be tuned easily by variation of substituents, there are also remarkable differences. The DPM anion shows more extensive charge delocalization over two linked five-membered rings whereas in the BDI anion the negative charge is delocalized only over the NCCCN backbone. Consequently, there is a higher negative charge on the N atoms in the BDI ligand which results in shorter metal-N bonds and thus wider N-metal-N bite angles.[9] The spreading of electron density over a larger area in DPM also makes this ligand less prone to electrophilic attack. Another major difference between DPM and BDI ligands is the arrangement of the sterically protecting substituents which, in the case of DPM, form a tight pocket around the metal (*cf.* angles in **VI** and **VII**).[9,10] This makes the DPM ligands especially useful for stabilizing monomeric complexes[11] or complexes with larger metal cations. We recently demonstrated that DPM ligands are able to stabilize heteroleptic (DPM)AeN(SiMe$_3$)$_2$ complexes with larger alkaline-earth (Ae) metals like Sr and Ba.[12]

Given the major successes of applying DPM as a ligand for boron in the famous BODIPY systems, and its ability to stabilize the coordination sphere of larger metals, it is remarkable that DPM ligands have been hardly employed in the chemistry of the heavier group 13 congeners Al and Ga. Apart from work by Mason and co-workers,[10] there is a rare application of (DPM)AlMe$_2$ as a cocatalyst in alkene polymerization in which role it functions as a fluorescent probe for investigation of active species in the polymerization mechanism.[13] In addition, as Ga compounds are useful for biomedical radiolabeling, a highly fluorescent (DPM)GaCl$_2$ complex, abbreviated as GADIPY, has been previously isolated.[14]

Scheme 1. Exemplary Ga^{I} Complexes and Geometrical Differences between Dipyrromethene (DPM) and β-Diketiminate (BDI) Ligands[a]

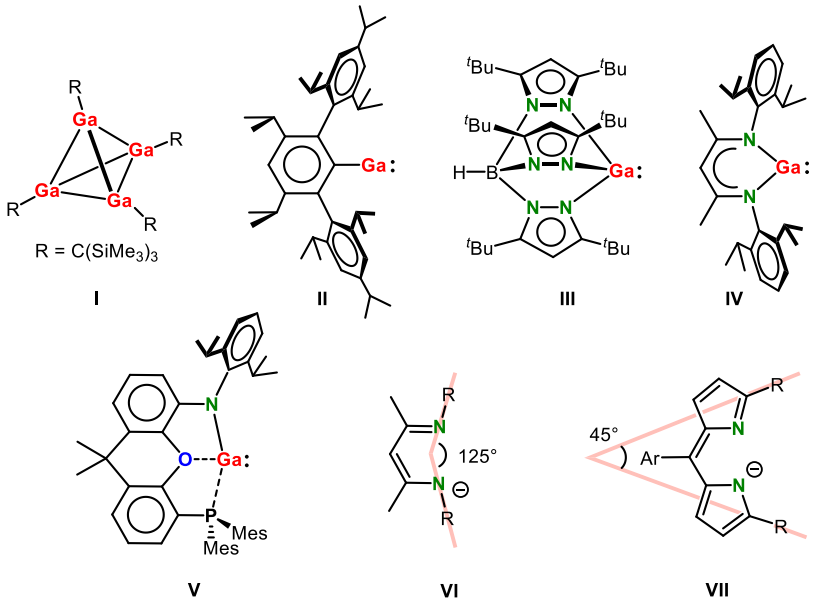

[a]The angles between the substituents in **VI** and **VII** are defined by the N-R and C-R axes, respectively.

Scheme 2. Syntheses of 1−4

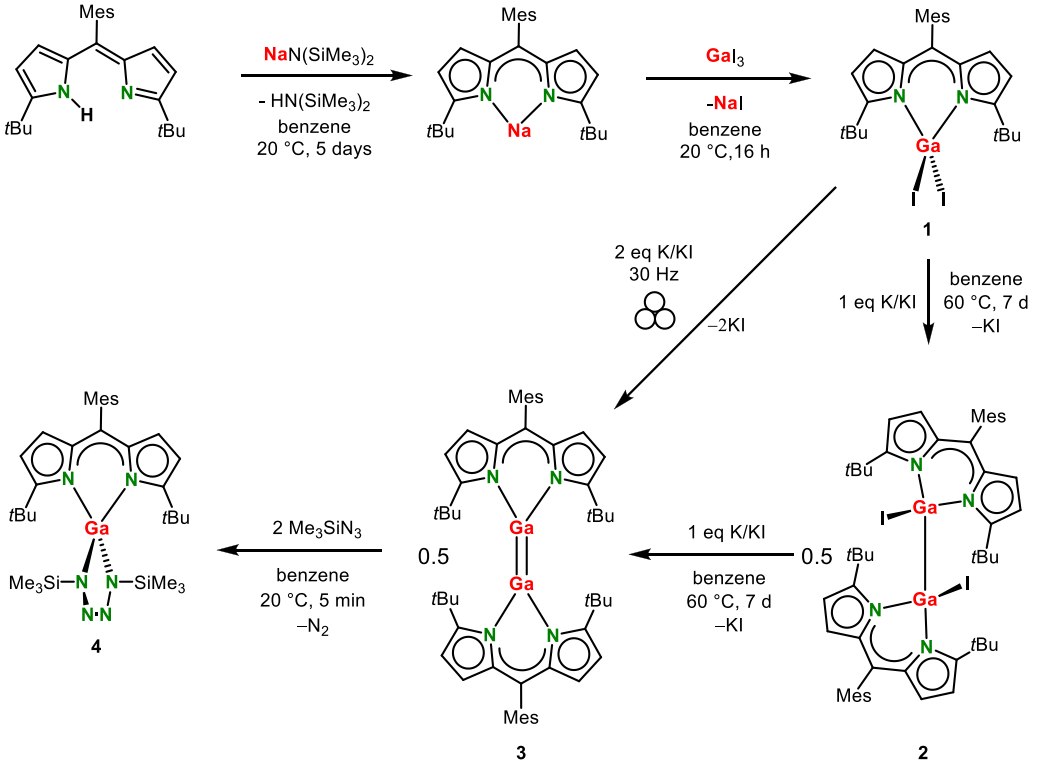

In this contribution we explore synthetic pathways to an $(DPM)Al^{I}$ complex, introduce a first DPM-stabilized Ga^{II} complex and exploit the encapsulating properties of the DPM ligand to stabilize a unique low-valent $(DPM)Ga^{I}$ complex for which we show preliminary reactivity.

RESULTS AND DISCUSSION

Synthesis and Reactivity. The DPM pro-ligand with protecting *t*Bu-substituents (^{tBu}DPM-H) was prepared according to Betley.[15] In an attempt to isolate low-valent $(^{tBu}DPM)Al^{I}$, the pro-ligand was deprotonated with $AlMe_3$ and the product $(^{tBu}DPM)AlMe_2$ was converted to $(^{tBu}DPM)AlI_2$ by reaction with I_2. All attempts to reduce the di-iodide precursor by reaction with KC_8 led to unselective conversions. Also the salt-metathesis route, $(AlCp^*)_4$ + $(^{tBu}DPM)Na$, gave a mixture of products which could not be purified. It is likely that the formation of a strongly reducing Al^{I} product results in reduction of the DPM ligand system. Since Ga^{I} complexes are generally

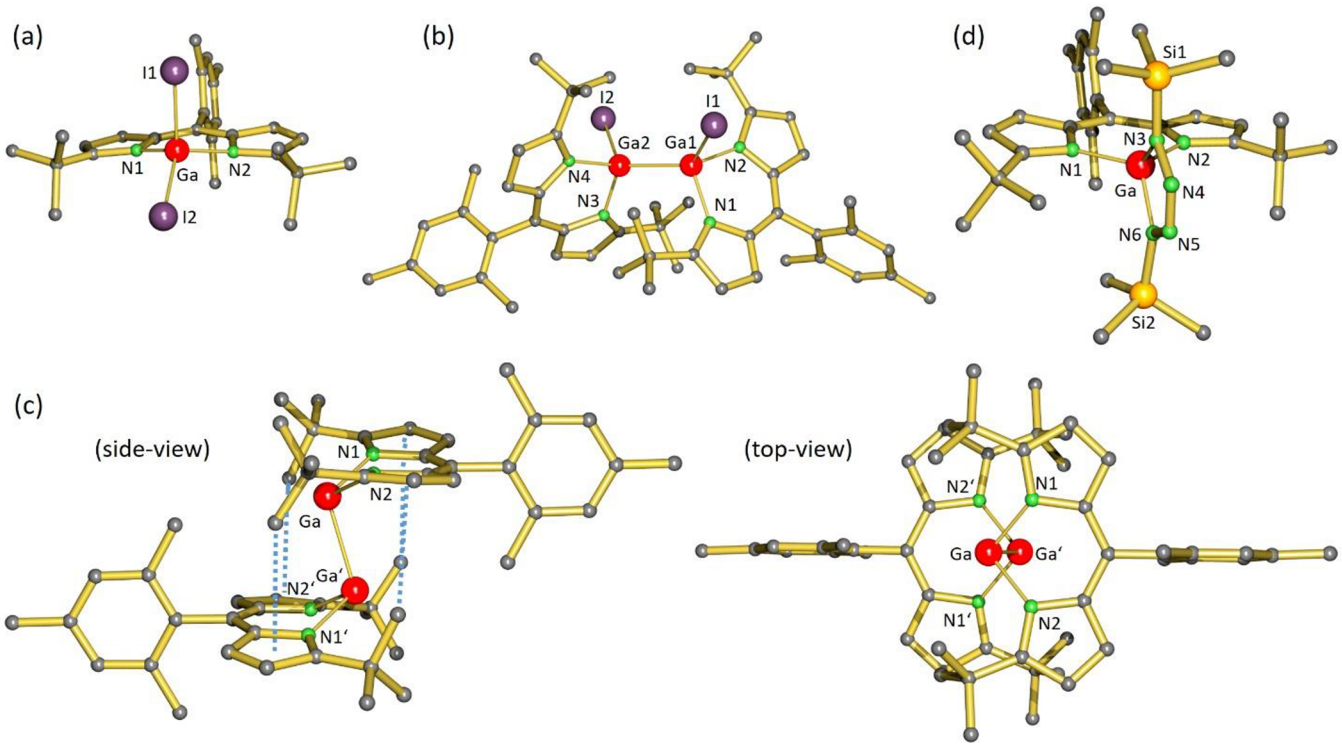

Figure 1. Crystal structures of (a) ($^{t\text{Bu}}$DPM)GaI$_2$ (**1**), (b) [($^{t\text{Bu}}$DPM)GaI]$_2$ (**2**), (c) two different views of [($^{t\text{Bu}}$DPM)Ga]$_2$ (**3**), and (d) ($^{t\text{Bu}}$DPM)Ga[N$_4$(SiMe$_3$)$_2$] (**4**). Hydrogen atoms have been omitted for clarity. Blue striped lines indicate dispersive Me-ring interactions.

less reactive than Al$^{\text{I}}$ complexes, we attempted syntheses of low-valent Ga species.

Stirring a solution of $^{t\text{Bu}}$DPM-H and NaN(SiMe$_3$)$_2$ in benzene for 5 days led to quantitative conversion to ($^{t\text{Bu}}$DPM)Na (Scheme 2). Subsequent salt-metathesis with GaI$_3$ gave ($^{t\text{Bu}}$DPM)GaI$_2$ (**1**) in an overall yield of 88%. Orange crystals suitable for X-ray diffraction studies were obtained from a benzene-hexanes mixture (the structure is discussed below).

The product ($^{t\text{Bu}}$DPM)GaI$_2$ could be considered as being isolobal to BODIPY complexes of general formula (DPM)BF$_2$. In accordance with it intensive orange color, it strongly absorbs green light (λ_{max} = 503 nm, ε_{max} = 1.62 × 10^5 L·mol^{-1}·cm^{-1}) and under UV light green fluorescence is observed (Figure S50).

Single reduction of ($^{t\text{Bu}}$DPM)GaI$_2$ (**1**) with only one equivalent of K/KI at 60 °C in benzene was complete after 7 days. Crystallization from a benzene-hexanes mixture gave [($^{t\text{Bu}}$DPM)GaI]$_2$ (**2**) in the form of intense orange crystals suitable for X-ray diffraction studies in a yield of 61% (the structure is discussed below). Also **2** absorbs strongly in the green area of the visible light spectrum (λ_{max} = 500 nm, ε_{max} = 1.69 × 10^5 L·mol^{-1}·cm^{-1}).

Double reduction of ($^{t\text{Bu}}$DPM)GaI$_2$ using two equivalents of K/KI in toluene at 60 °C produced a red suspension after 1 week. Following workup and crystallization from a toluene-hexanes mixture at −35 °C, dark-green crystals of [($^{t\text{Bu}}$DPM)-Ga]$_2$ (**3**) could be isolated in 40% yield (the structure is discussed below). When complex **3** is dissolved in toluene, an intensely red solution is formed (λ_{max} = 500 nm, ε_{max} = 5.28 × 10^4 L·mol^{-1}·cm^{-1}).

Complex **3** can be obtained faster and more selectively by a mechanochemical procedure. Ball-milling a mixture of solid ($^{t\text{Bu}}$DPM)GaI$_2$ and two equivalents of K/KI led to an orange powder after only 30 min. The KI salt was removed by toluene extraction which gave as a raw product essentially pure [($^{t\text{Bu}}$DPM)Ga]$_2$ (**3**) in a quantitative yield.

As the DPM ligand forms an encapsulating pocket around the metal, we attempted the isolation of a Ga-imido complex: ($^{t\text{Bu}}$DPM)Ga = N(SiMe$_3$). The reaction of [($^{t\text{Bu}}$DPM)Ga]$_2$ with two equivalents of Me$_3$SiN$_3$ was monitored by ^{1}H NMR which showed an immediate but partial conversion of only 50% of the Ga$^{\text{I}}$ reagent within five minutes. Reaction of [($^{t\text{Bu}}$DPM)Ga]$_2$ with four equivalents of Me$_3$SiN$_3$ showed complete and highly selective conversion within five minutes. Evaporation of all volatiles gave an orange powder as an essentially pure product in a quantitative yield. Crystals suitable for X-ray diffraction were grown from pentane at −35 °C and show selective formation of the tetrazagallole complex ($^{t\text{Bu}}$DPM)Ga[N$_4$(SiMe$_3$)$_2$] (**4**) (the structure is discussed below).

In comparison with literature, the selectivity in the formation of tetrazagallole complex **4** is remarkable. Reactions of low-valent Ga$^{\text{I}}$ complexes hitherto always resulted in the formation of at least two products: a tetrazagallole complex and an amido-azide complex with (Me$_3$Si)$_2$N$^-$ and N$_3^-$ ligands.[16,17] The sole formation of the tetrazagallole product is likely related to the steric influence of the DPM ligand which forms a pocket around the metal.

Crystal Structures. The crystal structure of ($^{t\text{Bu}}$DPM)GaI$_2$ (**1**, Figure 1a) compares well to those of reported (BDI)GaI$_2$ complexes.[16−18] There are, however, small differences. Although the Ga−N bond lengths in (BDI)GaI$_2$ complexes vary from 1.924(1) to 1.947(1) Å (average: 1.937 Å), those in **1** are slightly longer (1.951(2)-1.958(2) Å). This is in line with the somewhat weaker donor properties of DPM ligands compared to BDI ligands (*vide supra*). The Ga−I distances in **1** (2.5270(5)-2.5467(6) Å) are similar to those in BDI complexes and seemingly not affected by ligand choice. Like in the BDI complexes, one of the iodine ligands resides in the NCCCN

plane while the other is clearly located outside the plane. Also the Ga atom in **1** is located slightly above the NCCCN least-squares plane (0.439(1) Å). The DPM ligand deviates markedly from planarity (the two five-membered rings make an angle of 9.4(2)° with each other). In solution, however, the structure of **1** is fully C_{2v}-symmetric, indicating low energy fluxional behavior averaging the iodide positions. ^{1}H NMR shows one set of signals for both rings and one singlet for the *ortho*-Me groups of the mesitylene unit (Figure S15).

The crystal structure of $[(^{t\mathrm{Bu}}\mathrm{DPM})\mathrm{GaI}]_2$ (**2**) is close to being C_2-symmetric but there is no crystallographic symmetry (Figure 1b). It is comparable to a similar $[(\mathrm{BDI})\mathrm{GaI}]_2$ complex with 2,6-dimethylphenyl substituents at N (Scheme 3, **VIII**) which is

Scheme 3. Comparison of Ga–Ga distances (Å) in Ga^{II} complexes of type $[RGaI]_2$

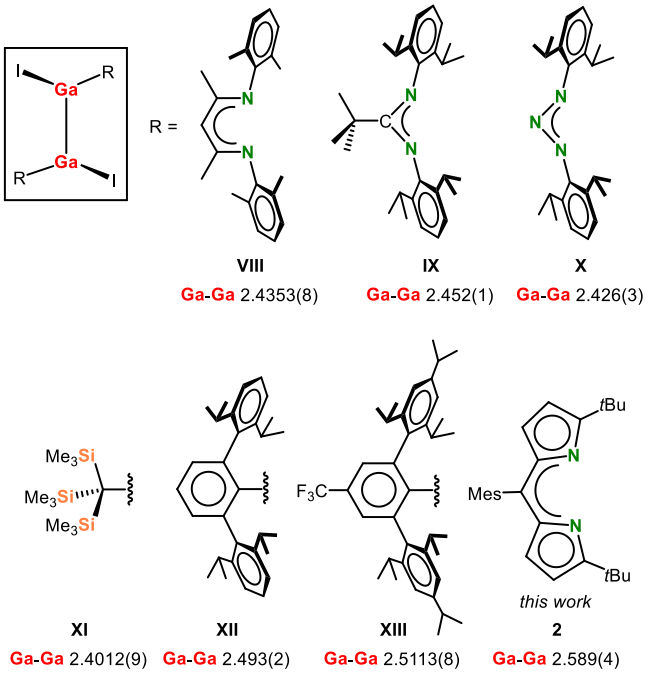

crystallographically C_2-symmetric.[19] The Ga–N bond lengths (1.993(9)-2.018(2) Å, average: 2.005 Å) are on average ca. 0.05 Å longer than those in **1**, which is in agreement with the decrease of oxidation state from + III to + II. They are also longer than those in the $[(\mathrm{BDI})\mathrm{GaI}]_2$ complex **VIII** (average: 1.960 Å)[19] which is in line with the weaker donor properties of the DPM ligand. While Ga–I distances in **2** (2.607(5)-2.6183(6) Å) are similar to that in $[(\mathrm{BDI})\mathrm{GaI}]_2$, the major difference between the comparable DPM and BDI complexes is in the Ga–Ga distances. The Ga–Ga distance of 2.589(4) Å in **2** is by far the longest distance measured in any Ga^{II} complex of type $[RGaI]_2$, also when compared to those complexes with other bidentate *N,N*-chelating ligands or bulky R groups (Scheme 3, **VIII**-**XIII**).[19–23] This illustrates the significant steric demand of DPM ligands. Dissolved in C_6D_6, complex **2** keeps its C_2-symmetric structure. This is evident from two sets of ^{1}H and ^{13}C NMR signals for the two five-membered rings and the two *ortho*-Me groups in the mesityl substituent.

Complex $[(^{t\mathrm{Bu}}\mathrm{DPM})\mathrm{Ga}]_2$ (**3**) crystallized in the centrosymmetric space group $P\bar{1}$ with a center of inversion on the Ga–Ga bond (Figure 1c). The DPM ligand is distorted from planarity and features a butterfly form with an interplanar angle of 16.9(1)° between the two five-membered rings. With an acute (Mes)C···Ga–Ga angle of 87.7(1)°, the molecule looks severely bent. However, since the Ga atom is displaced significantly outside the NCCCN least-squares plane (0.909(1) Å), the N–Ga–Ga angles are obtuse (104.1(1)°). The geometry of the complex has strong similarities to the typical *trans*-bent structures often observed for $R_2Sn{=}SnR_2$ complexes.[24] There is, however, a striking difference: although the *trans*-bent angles in dinuclear Sn^{II} complexes (angle between Sn–Sn bond and R-Sn-R plane) generally vary from 1.2 to 44.9°, complex **3** is extremely distorted from planarity, showing a very large *trans*-bent angle (angle between the Ga–Ga bond and the N–Ga–N plane) of 70.9(1)°. This extreme deformation is partially caused by the ligand geometry but also by dispersive interactions between the ligands. Each *t*Bu-substituent interacts with a five-membered heterocycle with C···ring-center distances down to 3.491(1) Å (see Figure 1c).

Reduction from Ga^{II} to Ga^{I} results in further increase of the Ga–N bond distances (**3**: 2.053(1)-2.056(1) Å). The average distances are Ga^{III}–N 1.955 Å (in **1**), Ga^{II}–N 2.005 Å (in **2**) and Ga^{I}–N 2.055 Å (in **3**). This shows that upon reducing the oxidation number by one unit, the Ga–N distances increase by 0.05 Å. Decrease in the metal oxidation state also influences the Ga–Ga bond length which increases from 2.589(4) Å in **2** to 2.6373(3) Å in **3**, i.e. also by approximately 0.05 Å. Although formally a Ga = Ga double bond, the interatomic distance between both Ga centers in **3** is large. It is larger than the Ga–Ga contacts (2.512(7)-2.6268(7) Å) measured in ArGaGaAr complexes with very bulky terphenyl ligands like in **XII**.[2,21] However, it is considerably shorter than the longest reported Ga–Ga contact of 2.787(1) Å in $[\mathrm{Ph_2P(N\text{-}DIPP)_2}]\mathrm{Ga}$–$\mathrm{Ga}[\mathrm{Ph_2P(N\text{-}DIPP)_2}]$ (DIPP = 2,6-diisopropylphenyl).[25] The observation that the latter complex also crystallizes in a monomeric form shows that the Ga–Ga bond is extremely weak. Indeed, calculations have shown that cleavage of the Ga–Ga bond in ArGaGaAr complexes only costs 5–8 kcal mol^{-1}.[2] This is in line with preference of the heavier group 13 metals for lone-pair character over π-bonding.[26] Metal–metal bond lengths are determined by other factors than electron sharing. Hence, the London dispersion interactions observed in **3** play an important role for its stability.

Dissolved in C_6D_6, complex **3** loses its *trans*-bent conformation. This is evident from one sharp singlet ^{1}H NMR signal for the *ortho*-Me groups in the mesityl substituent. ^{1}H NMR DOSY confirms that $[(^{t\mathrm{Bu}}\mathrm{DPM})\mathrm{Ga}]_2$ dissociates in highly symmetric mononuclear $(^{t\mathrm{Bu}}\mathrm{DPM})\mathrm{Ga}$ (see Supporting Information, Table S1). This shows that the Ga–Ga bond as found in the crystal structure of **3** is rather weak.

The tetrazagallole complex $(^{t\mathrm{Bu}}\mathrm{DPM})\mathrm{Ga}[\mathrm{N_4(SiMe_3)_2}]$ (**4**) crystallized as a monomer (Figure 1d). The Ga–N distances to the DPM ligand (1.957(1)-1.960(1) Å) compare to those in **1** and are typical for a Ga^{III} complex. The Ga–N distances to the $N_4(SiMe_3)_2$ ligand are much smaller (1.869(1)-1.873(1) Å) which is in line with the dianionic nature and the $(Me_3Si)N$–N = N–$N(SiMe_3)$ resonance structure of this ligand. The latter is supported by alternating long N–N (1.405(2) Å) and short N = N (1.269(2) Å) distances. The structure of $(^{t\mathrm{Bu}}\mathrm{DPM})\mathrm{Ga}$-$[\mathrm{N_4(SiMe_3)_2}]$ (**4**) shows a striking resemblance with that of the similar β-diketiminate complex $(\mathrm{BDI})\mathrm{Ga}[\mathrm{N_4(SiMe_3)_2}]$.[17] Like in the latter BDI complexes, a solution of **4** in C_6D_6 shows simple ^{1}H and ^{13}C NMR spectra. There is only one set of signals for both rings and the *ortho*-Me groups in the mesityl-substituent,

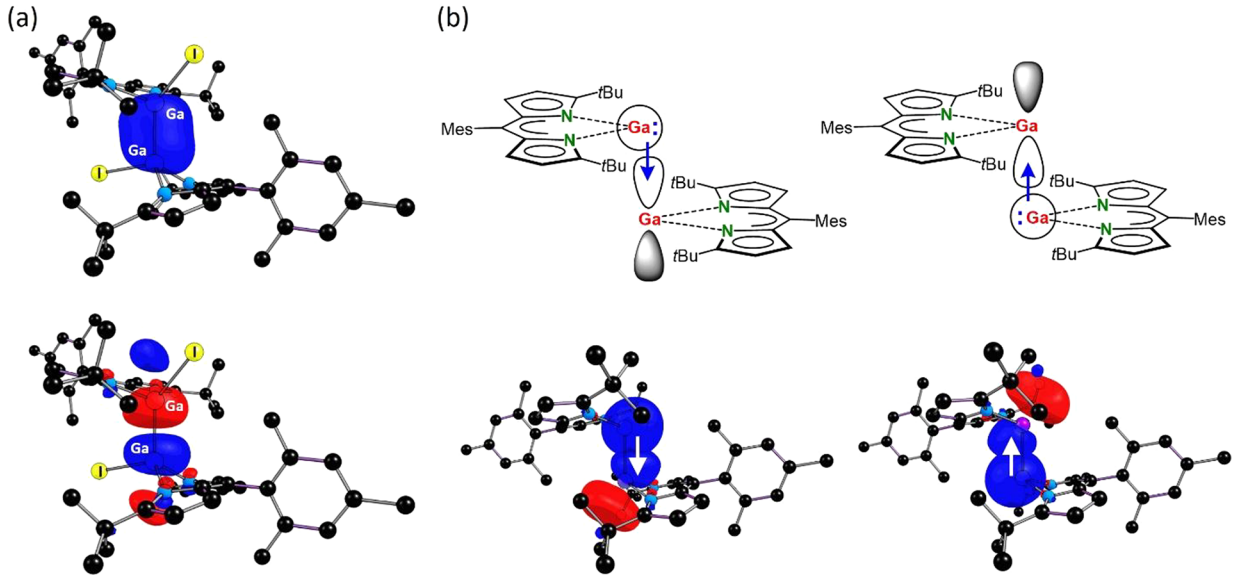

Figure 2. (a) NBO analysis of **2** shows a Ga−Ga bonding natural-bond-orbital with occupation of 1.90*e* (top) and an antibonding natural-bond-orbital with occupation 0.10*e* (bottom). (b) Double donor−acceptor bonding in complex **3** and the superimposed LP and LV NBOs for **3**, showing the donor−acceptor interactions.

indicating that the highly symmetric solid-state structure is retained in solution.

DFT Calculations. The bonding situations in **2** and **3** were investigated by Density Functional Theory (DFT), and subsequent Natural Bond Orbital (NBO) and Atoms-in-Molecules (AIM) analyses at the PBE0-D3BJ/Def2TZVP level of theory which include corrections for dispersion.

Complex **2** can be formally described as a Ga^{II} complex, bearing natural charges of +0.92/+0.93 at the two Ga centers. The Ga−Ga interaction is a single bond with a Wiberg Bond Index (WBI) of 0.83 and described with a bonding NBO containing 1.90 electrons which is essentially nonpolar, a complementary antibonding NBO is also observed accounting for the remaining 0.10 electrons in the interaction (Figure 2). The Kohn−Sham molecular orbitals are presented in the Supporting Information (Figures S58) and show that the HOMO−2 represent the bonding Ga−Ga interaction whereas the LUMO+2 represents the antibonding combination.

AIM analysis of **2** shows a bond-critical-point (bcp) on the Ga−Ga axis (Figure S56). The electron density $\rho(\mathbf{r})$ and Laplacian $\nabla^2\rho(\mathbf{r})$ in the bcp are 0.063 au and −0.051 au, respectively. These rather low values indicate a weak bond. Covalent bonds typically show large electron densities and negative Laplacians. Ionic bonds typically show small electron densities and positive Laplacians. The values for $\rho(\mathbf{r})$ and $\nabla^2\rho(\mathbf{r})$ in **2** show that weak Ga−Ga bonding is more covalent than ionic. The ellipticity index of 0.020 is typical for a cylindrical single bond.

On the contrary, the Ga^{I} complex (**3**) is best described as a double donor−acceptor complex, where a lone pair of electrons in each Ga is donating into a vacant *p*-orbital of the other Ga. The Wiberg Bond Index analysis gives a WBI of 0.99 for the Ga−Ga interaction, consistent with a single bond. However, NBO analysis shows no bonding interaction between the Ga centers that can be described as a Lewis structure. Instead, on each Ga atom a Ga lone pair (LP) is observed with 89.6% s-character, in addition to a valent lone vacant NBO (LV) with 98.1% p-character. Second-order perturbation theory analysis thus describes two donor−acceptor interactions between the LP and LV NBOs of the Ga centers with an energy of 72.5 kcal mol^{-1} (Figure 2). This can be further observed in the Kohn−Sham HOMO−3 (Figure S59). A more detailed analysis of Ga−Ga bond was recently reported by Krossing and co-workers.[27]

AIM analysis of **3** shows a bond-critical-point (bcp) on the Ga−Ga axis (Figure S57). The electron density $\rho(\mathbf{r})$ and Laplacian $\nabla^2\rho(\mathbf{r})$ in the bcp are 0.044 au and −0.007 au, respectively. The low electron density is consistent with a very weak Ga−Ga bond and explains why the dinuclear complex does not exist in solution. The Laplacian close to zero shows that there is very little electron accumulation between the Ga atoms. This is in agreement with facile Ga−Ga bond cleavage in **3** which only needs 4.9 kcal mol^{-1} (ΔG_{298}). The ellipticity index of 0.090 is typical for a cylindrical bond. This bond analysis shows that, although formally four electrons are involved in the Ga−Ga interaction, bonding between these metal atoms does not have the characteristics of a double bond as found in $H_2C{=}CH_2$ and is extremely weak. In fact, when we exclude dispersion corrections, complex **3** is unstable: cleavage into two (^{tBu}DPM)Ga monomers is exergonic by −2.7 kcal mol^{-1}).

Interested in unusual selectivity for formation of **4**, we investigated the mechanism by DFT (Figure 3). Reaction of $[(^{tBu}DPM)Ga]_2$ (**3**) with Me_3SiN_3 can be seen as a Staudinger-type reaction followed by a 1,3-dipolar cycloaddition. Starting with cleavage of **3** in two monomers (**3** → **A**, ΔG_{298} = +4.9 kcal mol^{-1}), the nucleophilic Ga^{I} center is able to undergo a concerted cyclization (**A** → **B**‡ → **C**, $\Delta G^{‡}_{298}$ = +16.3 kcal mol^{-1}) with the azide to form a four-membered GaNNN heterocycle with the Me_3Si-substituent perpendicular to the DPM-plane. From here, two thermally accessible pathways can be pursued toward the Ga-imido intermediate (**E**). (a) A direct elimination of dinitrogen (**C** → **D**‡ → **E**, $\Delta G^{‡}_{298}$ = +13.0 kcal mol^{-1}), or (b) rocking of the Me_3SiN_3 moiety so that the silane is now coplanar with DPM-plane (**C** → **F**‡ → **G**, $\Delta G^{‡}_{298}$ = +6.6 kcal mol^{-1}), followed by dinitrogen extrusion (**G** → **H**‡ → **E**, $\Delta G^{‡}_{298}$ = +6.9 kcal mol^{-1}); note that **C** and **G** differ only by the orientation of the Me_3Si-NNN unit in respect to the (DPM)Ga unit (see structures in Figure 3). The latter route is clearly more favorable. Starting from the Ga-imido intermediate (**E**), a second

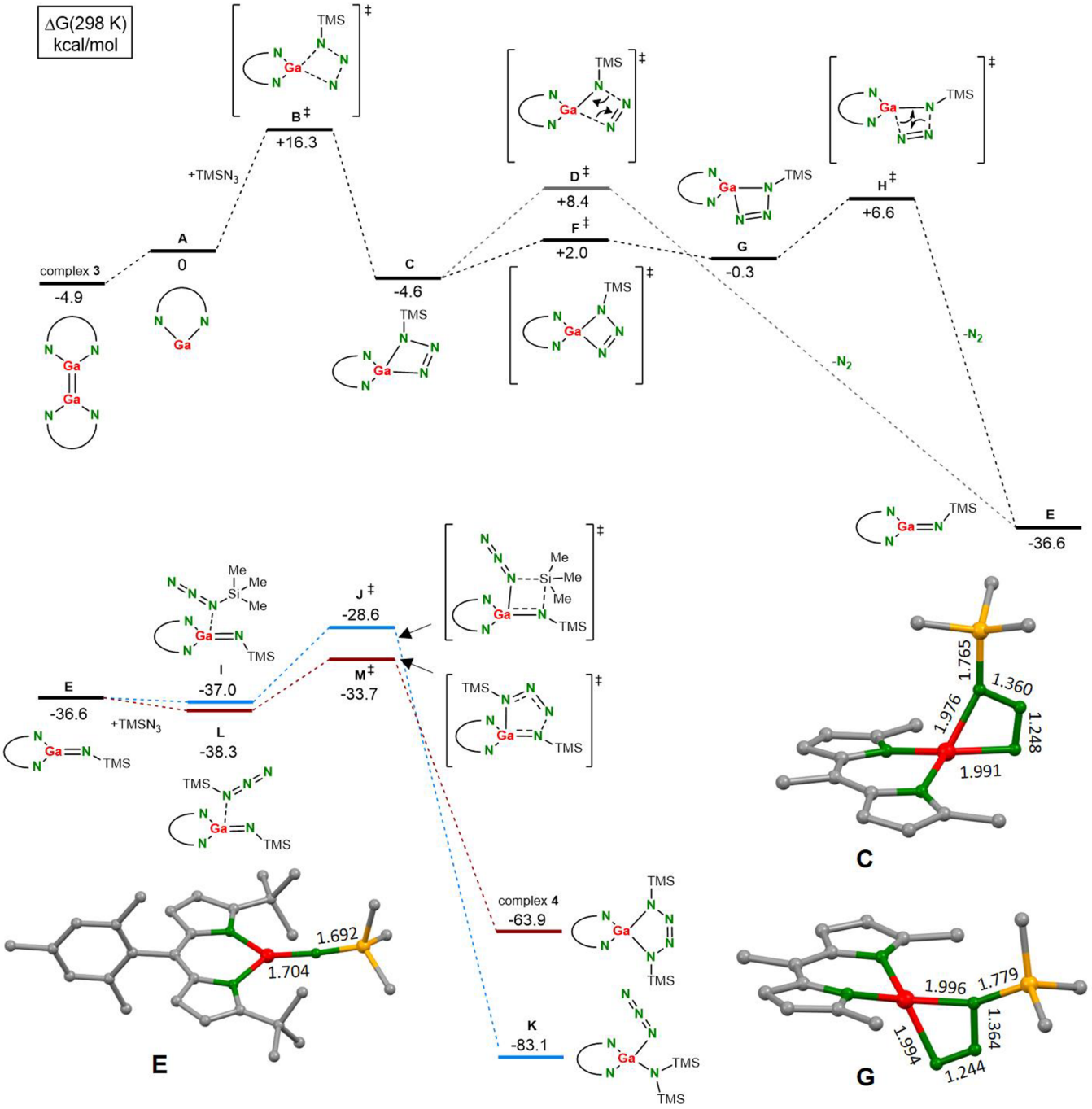

Figure 3. Energy profile for the reaction of complex **3** with Me_3SiN_3 ($\Delta G_{298\ K}$ in kcal mol^{-1}) and selected calculated structures for the proposed Ga-imido intermediates (^{tBu}DPM)Ga = N(SiMe$_3$) (**E**) and intermediates C and G (in the latter, the *t*Bu and xylyl-substituents are only partially shown for clarity).

equivalent of Me_3SiN_3 can react, first forming an adduct, with the Me_3Si-substituent either over the ligand backbone (**I**) or over the imido moiety (**L**). The latter conformation (**L**) was found to be 1.3 kcal mol^{-1} lower in energy, leading to tetrazagallole complex **O** by attack of the imido N at the terminal azide N. The other conformation (**J**) leads to attack of the imido nitrogen at Si and formation of the other possible product, the amide-azide combination **L**. As **L** (ΔG_{298} = −83.1 kcal mol^{-1}) is thermodynamically considerably more stable than the observed tetrazagallole product **4** ($\Delta G^{\ddagger}_{298}$ = −63.9 kcal mol^{-1}), the selective formation of **4** must be kinetically controlled. This is in agreement with a somewhat lower activation energy for formation of **4** (**L** → **M**‡ → **4**, $\Delta G^{\ddagger}_{298}$ = +4.6 kcal mol^{-1}) compared to that of **K** (**I** → **J**‡ → **K**, $\Delta G^{\ddagger}_{298}$ = +8.4 kcal mol^{-1}). Heating a solution of **4** did not lead to formation of **K**. This is typical for highly exothermic reactions that are kinetically controlled.

CONCLUSIONS

Attempted synthesis of the low-valent (^{tBu}DPM)Al^{I} complex failed and only decomposition products could be observed. Apparently, the highly reactive Al^{I} center is able to reduce the DPM ligand system. Since Ga^{I} complexes have larger HOMO−LUMO gaps than corresponding Al^{I} complexes, they are

considerably less reactive. This explains why ($^{t\mathrm{Bu}}$DPM)Ga$^{\mathrm{I}}$ could be prepared in a fair yield. The product crystallizes as [($^{t\mathrm{Bu}}$DPM)Ga$^{\mathrm{I}}$]$_2$ (**3**) but due to weak Ga−Ga bonding, the complex is mononuclear in benzene solution. DFT calculations and AIM analysis show that it is mainly held together by dispersive interactions between the DPM ligands. The very weak Ga−Ga bond in **3** should be described as a double donor−acceptor bond in which a pair of s-electrons from one Ga center is donated into an empty p-orbital on the other Ga center, and *vice versa*. We were also able to isolate the Ga$^{\mathrm{II}}$ complex [($^{t\mathrm{Bu}}$DPM)GaI]$_2$ (**2**) which is an intermediate in the reduction of ($^{t\mathrm{Bu}}$DPM)GaI$_2$ with K/KI. This complex also crystallizes as a digallane with a formal Ga−Ga single bond.

Attempts to isolate Ga-imido complex ($^{t\mathrm{Bu}}$DPM)Ga=N(SiMe$_3$) by reaction of [($^{t\mathrm{Bu}}$DPM)Ga$^{\mathrm{I}}$]$_2$ (**3**) with Me$_3$SiN$_3$ failed. This is due to the fact that $^{t\mathrm{Bu}}$DPM)Ga=N(SiMe$_3$) reacts faster with Me$_3$SiN$_3$ as **3**. Although one would expect major formation of the azide-amide combination ($^{t\mathrm{Bu}}$DPM)Ga(N$_3$)-[N(SiMe$_3$)$_2$], the tetrazagallole complex ($^{t\mathrm{Bu}}$DPM)Ga-[N$_4$(SiMe$_3$)$_2$] (**4**) formed selectively. This is likely due to the steric influence of the DPM ligand which forms a pocket around the metal. DFT calculations show that the azide-amide product is thermodynamically more stable but the transition state for tetrazagallole formation is ca. 5 kcal mol^{-1} lower in energy. This observation shows that constraining the coordination sphere around the metal by use of DPM ligands can have clear advantages in chemical conversions.

EXPERIMENTAL SECTION

All experiments were conducted under an inert atmosphere by applying standard Schlenk techniques or using nitrogen-filled gloveboxes (MBraun, Labmaster SP). Benzene, hexanes, *n*-pentane, and toluene were degassed with nitrogen, dried over activated aluminum oxide (Innovative Technology, Pure Solv 400−4-MD, Solvent Purification System), and stored under inert atmosphere over molecular sieves (3 Å). Benzene-d$_6$ (Sigma-Aldrich) and toluene-d$_8$ (Sigma-Aldrich) were dried over 3 Å molecular sieves. Elemental iodine (99+%, Acros Organics) was sublimed prior to use and stored under nitrogen atmosphere. Gallium(III) triiodide (99%, abcr), potassium (chunks, washed with hexanes, 98% trace metal basis, Sigma-Aldrich), potassium iodide (>99.5%, TCI Chemicals), sodium *bis*(trimethylsilyl)amide (95%, Sigma-Aldrich), and trimethylsilyl azide (95%, abcr) were purchased as indicated and used without further purification. The protio-ligand 1,9-di(*t*-butyl)-5-mesityldipyrromethene, ($^{t\mathrm{Bu}}$DPM)H,[15] and K/KI[28] were prepared according to literature procedures. NMR spectra were recorded with a Bruker Avance III HD 600 MHz NMR spectrometer. Chemical shifts (δ) were reported in parts per million (ppm) and the spectra were referenced to solvent residual signal. Coupling constants (J) were given in Hertz (Hz). Details for DOSY NMR measurements are described in the Supporting Information.

Elemental analysis was performed with a Hekatech Eurovector EA 3000 Analyzer. All crystal structures were measured on a SuperNova diffractometer with dual Cu and Mo microfocus sources and an Atlas S2 detector.

Ball-milling experiments were performed with an ULTRA-TURRAX Tube Drive P control from IKA using 20 mL polypropylene vessels with three stainless steel balls (diameter: 5 mm, weight: 0.52 g, type: AISI 304).

UV−vis absorption spectra were acquired on a Cary 5 Spectrophotometer. Crystallographic data have been deposited with the Cambridge Crystallographic Data Centre as supplementary publication numbers: CCDC 2343806 ($^{t\mathrm{Bu}}$DPM)GaI$_2$ (**1**), 2343807 [($^{t\mathrm{Bu}}$DPM)-GaI]$_2$ (**2**), 2343808 [($^{t\mathrm{Bu}}$DPM)Ga]$_2$ (**3**), 2343809 ($^{t\mathrm{Bu}}$DPM)Ga-[N$_4$(SiMe$_3$)$_2$] (**4**), 2343810 ($^{t\mathrm{Bu}}$DPM)AlMe$_2$.

($^{t\mathrm{Bu}}$DPM)AlMe$_2$. $^{t\mathrm{Bu}}$DPM-H (100 mg, 267 μmol, 1.00 equiv) was dissolved in benzene (3 mL). The yellow solution instantly turned brown when AlMe$_3$ (20.2 mg, 280 μmol, 1.05 equiv) was added. The mixture was stirred at room temperature overnight. The solvent and excess AlMe$_3$ were removed *in vacuo*. The product was dried and obtained as an orange-brown solid (106 mg, 264 μmol, 99%). The dissolved product is green fluorescent in solution. Orange crystals suitable for X-ray diffraction analysis were grown from a saturated hexanes solution at −35 °C.

^{1}H NMR (C$_6$D$_6$, 600 MHz, 298 K): δ = 6.73 (s, 2H, aryl-*H*), 6.66 (d, J = 4.3 Hz, 2H, pyrrole-*H*), 6.37 (d, J = 4.4 Hz, 2H, pyrrole-*H*), 2.17 (s, 3H, *para*-C$_6$H$_2$(C*H*$_3$)$_3$), 2.07 (s, 6H, *ortho*-C$_6$H$_2$(C*H*$_3$)$_3$), 1.45 (s, 18H, C(C*H*$_3$)$_3$), 0.14 (s, 6H, Al(C*H*$_3$)$_2$) ppm.

^{13}C NMR (C$_6$D$_6$, 151 MHz, 298 K): δ = 173.4 (aryl-*C*), 145.2 (aryl-*C*), 138.4 (aryl-*C*), 137.5 (aryl-*C*), 136.9 (aryl-*C*), 136.1 (pyrrole-*C*), 133.0 (pyrrole-*C*H), 128.2 (aryl-*C*H), 117.9 (pyrrole-*C*H), 34.9 (*C*(CH$_3$)$_3$), 31.5 (C(*C*H$_3$)$_3$), 21.1 (C$_6$H$_2$(*C*H$_3$)$_3$), 19.9 (C$_6$H$_2$(*C*H$_3$)$_3$) ppm. Al(*C*H$_3$)$_2$ signal is not observed.

Elemental Analysis. Calculated values (%) for C$_{28}$H$_{39}$N$_2$Al (430.62 g/mol): C 78.10, H 9.13, N 6.51; Found (%): C 78.10, H 9.03, N 6.69.

($^{t\mathrm{Bu}}$DPM)AlI$_2$. ($^{t\mathrm{Bu}}$DPM)AlMe$_2$ (34.1 mg, 79.3 μmol, 1.00 equiv) was dissolved in benzene-d$_6$ (600 μL). I$_2$ (41.3 mg, 163 μmol, 2.05 equiv) was added. The mixture was stirred for 3 days at room temperature. The solvent was removed *in vacuo* and dried. The product was obtained as a red solid. Red microcrystals were grown from a saturated toluene solution by vapor diffusion with hexanes at −35 °C (15.4 mg, 23.5 μmol, 30%).

^{1}H NMR (C$_6$D$_6$, 600 MHz, 298 K): δ = 7.94 (s, 2H, aryl-*H*), 6.71 (s, 2H, pyrrole-*H*), 6.62 (s, 2H, pyrrole-*H*), 2.08 (s, 3H, *para*-C$_6$H$_2$(C*H*$_3$)$_3$), 2.04 (s, 6H, *ortho*-C$_6$H$_2$(C*H*$_3$)$_3$), 0.82 (s, 18H, C(C*H*$_3$)$_3$) ppm.

^{13}C NMR (C$_6$D$_6$, 151 MHz, 298 K): δ = 147.4 (aryl-*C*), 147.2 (aryl-*C*), 139.8 (aryl-*C*), 138.5 (aryl-*C*), 138.4 (aryl-*C*), 136.9 (aryl-*C*), 136.8 (aryl-*C*), 136.4 (aryl-*C*H), 136.3 (pyrrole-*C*H), 133.6 (aryl-*C*), 128.5 (aryl-*C*H), 128.2 (aryl-*C*), 128.1 (aryl-*C*), 127.9 (aryl-*C*), 118.5 (pyrrole-*C*), 35.4 (*C*(CH$_3$)$_3$), 32.3 (C(*C*H$_3$)$_3$), 32.2 (*C*(CH$_3$)$_3$), 30.9 (C(*C*H$_3$)$_3$), 21.0 (C$_6$H$_2$(*C*H$_3$)$_3$), 20.9 (C$_6$H$_2$(*C*H$_3$)$_3$), 20.0 (C$_6$H$_2$(*C*H$_3$)$_3$), 20.0 (C$_6$H$_2$(*C*H$_3$)$_3$) ppm.

($^{t\mathrm{Bu}}$DPM)GaI$_2$ (1). $^{t\mathrm{Bu}}$DPM-H (405 mg, 1.08 mmol, 1.00 equiv) was dissolved in benzene (15 mL). NaN(SiMe$_3$)$_2$ (297 mg, 1.62 mmol, 1.50 equiv) was added to the solution. The brown suspension was stirred at room temperature for 5 days, while the color turned orange (attempts to accelerate conversion by using higher temperatures or KN(SiMe$_3$)$_2$ led to formation of side-products). The mixture was filtered, the solvent was removed under reduced pressure, and the precipitate was washed with hexanes (2 × 10 mL). After drying *in vacuo*, the resulting yellow-orange powder of ($^{t\mathrm{Bu}}$DPM)Na was redissolved in benzene (10 mL). GaI$_3$ (486 mg, 1.08 mmol, 1.00 equiv) was added to the solution. The orange reaction mixture was stirred at room temperature overnight. The mixture was filtered, the solvent was removed under reduced pressure, and the precipitate was dried *in vacuo* to obtain essentially pure ($^{t\mathrm{Bu}}$DPM)GaI$_2$ as an orange powder (661 mg, 947 μmol, 88%). Orange crystals suitable for X-ray diffraction analysis were grown from a saturated benzene solution layered with hexanes at 60 °C.

^{1}H NMR (C$_6$D$_6$, 600 MHz, 298 K): δ = 6.68 (s, 2H, aryl-*H*), 6.57 (d, J = 4.4 Hz, 2H, pyrrole-*H*), 6.29 (d, J = 4.4 Hz, 2H, pyrrole-*H*), 2.14 (s, 3H, *para*-C$_6$H$_2$(C*H*$_3$)$_3$), 2.00 (s, 6H, *ortho*-C$_6$H$_2$(C*H*$_3$)$_3$), 1.67 (s, 18H, C(C*H*$_3$)$_3$) ppm.

^{13}C{^{1}H} NMR (C$_6$D$_6$, 151 MHz, 298 K): δ = 175.0 (aryl-*C*), 144.4 (aryl-*C*), 138.1 (aryl-*C*), 137.2 (aryl-*C*), 137.0 (aryl-*C*), 134.3 (pyrrole-*C*H), 128.3 (aryl-*C*H), 127.9 (aryl-*C*), 119.1 (pyrrole-*C*H), 35.9 (*C*(CH$_3$)$_3$), 32.8 (C(*C*H$_3$)$_3$), 21.1 (C$_6$H$_2$(*C*H$_3$)$_3$), 19.9 (C$_6$H$_2$(*C*H$_3$)$_3$) ppm.

^{71}Ga NMR (183 MHz, 298 K, C$_6$D$_6$): δ = −12.3 (*Ga*I$_2$) ppm (referenced to Ga(NO$_3$)$_3$ in D$_2$O).

Elemental Analysis. Calculated values (%) for C$_{26}$H$_{33}$N$_2$GaI$_2$ (697.10 g/mol): C 44.80, H 4.77, N 4.02; Found (%): C 45.78, H 4.84, N 3.77. Although these results are outside the range viewed as establishing analytical purity, they are provided to illustrate the best values obtained to date.

UV/vis (Toluene, 22 °C). λ (in nm) [ε (in L · mol^{-1} · cm^{-1})] = 478 [3.76 × 10^4], 503 [1.62 × 10^5].

[($^{t\mathrm{Bu}}$DPM)GaI]$_2$ (2). ($^{t\mathrm{Bu}}$DPM)GaI$_2$ (30.0 mg, 43.0 μmol, 1.00 equiv) was dissolved in benzene (600 μL) in a Schlenk tube. K/KI (5% w/w, 35.3 mg, 45.2 μmol, 1.05 equiv) was added to the solution. The reaction mixture was stirred at 60 °C for 7 days giving an orange suspension. The mixture was filtered, the solvent was removed under reduced pressure, and the precipitate was dried *in vacuo* to obtain [($^{t\mathrm{Bu}}$DPM)GaI]$_2$ as an orange powder. Orange crystals suitable for X-ray diffraction analysis were grown from a saturated benzene solution by vapor diffusion with hexanes at room temperature (15.0 mg, 13.2 μmol, 61%).

^{1}H NMR (C_6D_6, 600 MHz, 298 K): δ = 6.84 (s, 2H, Mes-*H*), 6.69–6.68 (m, 4H, Mes/pyrrole-*H*), 6.63 (d, J = 4.3 Hz, 2H, pyrrole-*H*), 6.41 (d, J = 4.5 Hz, 2H, pyrrole-*H*), 6.21 (d, J = 4.3 Hz, 2H, pyrrole-*H*), 2.25 (s, 6H, $C_6H_2(CH_3)_3$), 2.20 (s, 6H, $C_6H_2(CH_3)_3$), 2.10 (s, 6H, $C_6H_2(CH_3)_3$), 1.92 (s, 18H, $C(CH_3)_3$), 1.41 (s, 18H, $C(CH_3)_3$) ppm.

^{13}C{^{1}H} NMR (C_6D_6, 151 MHz, 298 K): δ = 174.8 (aryl-*C*), 172.6 (aryl-*C*), 143.6 (aryl-*C*), 138.8 (aryl-*C*), 137.7 (aryl-*C*), 137.0 (aryl-*C*), 136.2 (pyrrole-*C*), 136.2 (pyrrole-*C*), 135.7 (pyrrole-*C*), 134.0 (pyrrole-CH), 133.2 (pyrrole-CH), 128.6 (pyrrole-CH), 127.8 (pyrrole-CH), 119.4 (pyrrole-CH), 118.3 (pyrrole-CH), 41.7 ($C(CH_3)_3$), 36.4 ($C(CH_3)_3$), 36.4 ($C(CH_3)_3$), 35.7 ($C(CH_3)_3$), 35.0 ($C(CH_3)_3$), 34.9 ($C(CH_3)_3$), 33.7 ($C(CH_3)_3$), 32.1 ($C(CH_3)_3$), 29.6 ($C(CH_3)_3$), 29.4 ($C(CH_3)_3$), 28.0 ($C(CH_3)_3$), 27.3 ($C(CH_3)_3$), 25.7 ($C(CH_3)_3$), 23.0 ($C(CH_3)_3$), 22.8 ($C_6H_2(CH_3)_3$), 21.2 ($C_6H_2(CH_3)_3$), 21.1 ($C_6H_2(CH_3)_3$), 20.9 ($C_6H_2(CH_3)_3$), 20.9 ($C_6H_2(CH_3)_3$), 20.2 ($C_6H_2(CH_3)_3$), 19.6 ($C_6H_2(CH_3)_3$), 19.0 ($C_6H_2(CH_3)_3$) ppm.

^{71}Ga NMR (183 MHz, 298 K, C_6D_6): Not observed.

Elemental Analysis. Calculated values (%) for $C_{52}H_{66}N_4Ga_2I_2$ (1140.38 g/mol): C 54.77, H 5.83, N 4.91; Found (%): C 55.53, H 5.41, N 5.53. Although these results are outside the range viewed as establishing analytical purity, they are provided to illustrate the best values obtained to date.

UV/vis (Toluene, 22 °C). λ (in nm) [ε (in L · mol^{-1} · cm^{-1})] = 474 [4.40 × 10^4], 500 [1.69 × 10^5].

[($^{t\mathrm{Bu}}$DPM)Ga]$_2$ (3). ($^{t\mathrm{Bu}}$DPM)GaI$_2$ (100 mg, 143 μmol, 1.00 equiv) was dissolved in toluene (600 μL) in a Schlenk tube. K/KI (5% w/w, 236 mg, 301 μmol, 2.10 equiv) was added to the solution. The orange reaction mixture was stirred at 60 °C for 7 days giving a red suspension. The mixture was filtered, the solvent was removed under reduced pressure, and the precipitate was dried *in vacuo*. Dark-green crystals of [($^{t\mathrm{Bu}}$DPM)Ga]$_2$ (12.5 mg, 28.2 μmol, 40%) suitable for X-ray diffraction analysis were grown from a saturated toluene solution by vapor diffusion with hexanes at −35 °C.

Alternatively, ($^{t\mathrm{Bu}}$DPM)GaI$_2$ (69.7 mg, 100 μmol, 1.00 equiv) and K/KI (5% w/w, 164 mg, 210 μmol, 2.10 equiv) were mixed in a ball mill vessel equipped with three stainless steel balls. The reaction mixture was ground at room temperature for 30 min with a ball mill speed of 30 Hz. After extraction of the resulting orange powder with toluene, the mixture was filtered, the solvent was removed under reduced pressure, and the precipitate was dried *in vacuo* to obtain essentially pure orange-red powder [($^{t\mathrm{Bu}}$DPM)Ga]$_2$ in a quantitative yield.

Another alternative route involved the [($^{t\mathrm{Bu}}$DPM)GaI]$_2$ complex: [($^{t\mathrm{Bu}}$DPM)GaI]$_2$ (31.9 mg, 28.0 μmol, 1.00 equiv) was dissolved in benzene (600 μL) in a Schlenk tube. K/KI (5% w/w, 46.0 mg, 58.8 μmol, 2.10 equiv) was added to the solution. The reaction mixture was stirred at 60 °C for 7 days giving an orange suspension. The mixture was filtered, the solvent was removed under reduced pressure, and the precipitate was dried *in vacuo* to obtain essentially pure [($^{t\mathrm{Bu}}$DPM)Ga]$_2$ as an orange-red powder in quantitative yield.

^{1}H NMR (C_6D_6, 600 MHz, 298 K): δ = 6.79 (s, 2H, Mes-*H*), 6.65 (d, J = 4.1 Hz, 2H, pyrrole-*H*), 6.30 (d, J = 4.1 Hz, 2H, pyrrole-*H*), 2.19 (s, 9H, $C_6H_2(CH_3)_3$), 1.51 (s, 18H, $C(CH_3)_3$) ppm.

^{13}C{^{1}H} NMR (C_6D_6, 151 MHz, 298 K): δ = 173.0 (aryl-*C*), 145.6 (aryl-*C*), 137.3 (aryl-*C*), 137.2 (aryl-*C*), 137.1 (aryl-*C*), 135.9 (pyrrole-*C*), 131.5 (pyrrole-CH), 128.4 (aryl-CH), 128.2 (Mes-CH), 115.9 (pyrrole-CH), 35.0 ($C(CH_3)_3$), 32.1 ($C(CH_3)_3$), 21.2 ($C_6H_2(CH_3)_3$), 20.3 ($C_6H_2(CH_3)_3$) ppm.

^{71}Ga NMR (183 MHz, 298 K, C_6D_6): Not observed.

Elemental Analysis. Calculated values (%) for $C_{52}H_{66}Ga_2N_4$ (886.58 g/mol): C 70.45, H 7.50, N 6.32; Found (%): C 69.80, H 7.40, N 5.98. Although these results are outside the range viewed as establishing analytical purity, they are provided to illustrate the best values obtained to date.

UV/vis (Toluene, 22 °C). λ (in nm) [ε (in L·mol^{-1}·cm^{-1})] = 448 [1.90 × 10^4], 476 [2.53 × 10^4], 500 [5.28 × 10^4].

($^{t\mathrm{Bu}}$DPM)Ga(N$_4$TMS$_2$) (4). [($^{t\mathrm{Bu}}$DPM)Ga]$_2$ (**3**) (10.0 mg, 11.3 μmol, 1.00 equiv) was dissolved in benzene-d$_6$ (600 μL) in a J.-Young NMR tube. Trimethylsilyl azide (5.21 mg, 45.2 μmol, 4.00 equiv) was added at room temperature. The reaction was finished immediately as indicated by ^{1}H NMR spectroscopy. The solvent was removed under reduced pressure, and the residue was dried *in vacuo* to obtain ($^{t\mathrm{Bu}}$DPM)Ga(N$_4$TMS$_2$) as an orange powder (13.8 mg, 21.4 μmol, 95%). Orange crystals suitable for X-ray diffraction analysis were grown from a saturated *n*-pentane solution at −35 °C.

^{1}H NMR (C_6D_6, 600 MHz, 298 K): δ = 6.74 (s, 2H, Mes-*H*), 6.57 (s, 2H, pyrrole-*H*), 6.31 (s, 2H, pyrrole-*H*), 2.19 (d, J = 2.3 Hz, 3H, *para*-$C_6H_2(CH_3)_3$), 2.07 (d, J = 2.4 Hz, 6H, *ortho*-$C_6H_2(CH_3)_3$), 1.28–1.24 (m, 18H, $C(CH_3)_3$), 0.41–0.37 (m, 18H, TMS–CH_3) ppm.

^{13}C{^{1}H} NMR (C_6D_6, 151 MHz, 298 K): δ = 176.6 (aryl-*C*), 144.0 (pyrrole-*C*), 138.6 (pyrrole-*C*), 138.1 (aryl-*C*), 136.8 (aryl-*C*), 135.7 (pyrrole-*C*), 134.0 (aryl-*C*), 128.4 (aryl-CH), 128.3 (aryl-CH), 119.5 (pyrrole-CH), 35.7 ($C(CH_3)_3$), 31.5 ($C(CH_3)_3$), 21.1 ($C_6H_2(CH_3)_3$), 19.7 ($C_6H_2(CH_3)_3$), 1.2 (TMS-CH_3) ppm.

^{29}Si NMR (C_6D_6, 119 MHz, 298 K): δ = 5.40 (TMS) ppm.

^{71}Ga NMR (183 MHz, 298 K, C_6D_6): Not observed.

Elemental Analysis. Calculated values (%) for $C_{32}H_{51}N_6GaSi_2$ (645.70 g/mol): C 59.53, H 7.96, N 13.02; Found (%): C 58.51, H 7.15, N 11.63. Although these results are outside the range viewed as establishing analytical purity, they are provided to illustrate the best values obtained to date.

ASSOCIATED CONTENT

Accession Codes

CCDC 2343806–2343810 contain the supplementary crystallographic data for this paper. These data can be obtained free of charge via www.ccdc.cam.ac.uk/data_request/cif, or by emailing data_request@ccdc.cam.ac.uk, or by contacting The Cambridge Crystallographic Data Centre, 12 Union Road, Cambridge CB2 1EZ, UK; fax: +44 1223 336033.

AUTHOR INFORMATION

Corresponding Author

Sjoerd Harder − *Inorganic and Organometallic Chemistry, Friedrich-Alexander-Universität Erlangen-Nürnberg, 91058 Erlangen, Germany*; orcid.org/0000-0002-3997-1440; Email: sjoerd.harder@fau.de

Authors

Tim Richter − *Inorganic and Organometallic Chemistry, Friedrich-Alexander-Universität Erlangen-Nürnberg, 91058 Erlangen, Germany*

Stefan Thum − *Inorganic and Organometallic Chemistry, Friedrich-Alexander-Universität Erlangen-Nürnberg, 91058 Erlangen, Germany*

Timothy Vilpas − *Inorganic and Organometallic Chemistry, Friedrich-Alexander-Universität Erlangen-Nürnberg, 91058 Erlangen, Germany*

Oliver P. E. Townrow − *Inorganic and Organometallic Chemistry, Friedrich-Alexander-Universität Erlangen-Nürnberg, 91058 Erlangen, Germany;* orcid.org/0000-0001-9556-6450

Lukas Klerner − *Inorganic and Organometallic Chemistry, Friedrich-Alexander-Universität Erlangen-Nürnberg, 91058 Erlangen, Germany*

Jens Langer − *Inorganic and Organometallic Chemistry, Friedrich-Alexander-Universität Erlangen-Nürnberg, 91058 Erlangen, Germany;* orcid.org/0000-0002-2895-4979

Notes

The authors declare no competing financial interest.

ACKNOWLEDGMENTS

We acknowledge A. Roth (University of Erlangen-Nürnberg) for CHN analyses, J. Schmidt and Dr. C. Färber (University of Erlangen-Nürnberg) for assistance with the NMR analyses and M. Reil for assistance with UV−vis spectroscopy.

REFERENCES

(1) Uhl, W.; Hiller, W.; Layh, M.; Schwarz, W. $[Ga_4\{C(SiMe_3)_3\}_4]$ with a Tetrahedral Ga_4 Skeleton. *Angew. Chem., Int. Ed. Engl.* **1992**, *31*, 1364−1366.

(2) Zhu, Z.; Fischer, R. C.; Ellis, B. D.; Rivard, E.; Merrill, W. A.; Olmstead, M. M.; Power, P. P.; Guo, J. D.; Nagase, S.; Pu, L. Synthesis, Characterization and Real Molecule DFT Calculations for Neutral Organogallium(I) Aryl Dimers and Monomers: Weakness of Gallium-Gallium Bonds in Digallenes and Digallynes. *Chem. Eur. J.* **2009**, *15*, 5263−5272.

(3) Hardman, N. J.; Eichler, B. E.; Power, P. P. Synthesis and Characterization of the Monomer $Ga\{(NDippCMe)_2CH\}$ (Dipp = $C_6H_3Pri_2$-2,6): A Low Valent Gallium(I) Carbene Analogue. *Chem. Commun.* **2000**, *20*, 1991−1992.

(4) Zheng, X.; Heilmann, A.; McManus, C.; Aldridge, S. A Xanthene-Based Mono-Anionic PON Ligand: Exploiting a Bulky, Electronically Unsymmetrical Donor in Main Group Chemistry. *Chem. Eur. J.* **2021**, *27*, 3159−3165.

(5) Kuchta, M. C.; Bonanno, J. B.; Parkin, G. A Monovalent Gallium Complex Supported by Tris(3,5-Di-Tert-Butylpyrazolyl)Hydroborato Ligation: The Syntheses and Structures of $[TpBut_2]Ga$ and Its GaI_3 Adduct, $[TpBut_2]Ga{\rightarrow}GaI_3$[1]. *J. Am. Chem. Soc.* **1996**, *118*, 10914−10915.

(6) Zhong, M.; Sinhababu, S.; Roesky, H. W. The Unique β-Diketiminate Ligand in Aluminum(I) and Gallium(I) Chemistry. *Dalton Trans.* **2020**, *49*, 1351−1364.

(7) Fischer, H.; Schubert, M. Synthetische Versuche mit Blutfarbstoff-Spaltprodukten und Komplexsalz-Bildung bei Dipyrryl-methenen (II.). *Berichte Dtsch. Chem. Ges. B Ser.* **1924**, *57*, 610−617.

(8) Loudet, A.; Burgess, K. BODIPY Dyes and Their Derivatives: Syntheses and Spectroscopic Properties. *Chem. Rev.* **2007**, *107*, 4891−4932.

(9) Ballmann, G.; Grams, S.; Elsen, H.; Harder, S. Dipyrromethene and β-Diketiminate Zinc Hydride Complexes: Resemblances and Differences. *Organometallics* **2019**, *38*, 2824−2833.

(10) Gianopoulos, C. G.; Kirschbaum, K.; Mason, M. R. Mono- and Bimetallic Aluminum Alkyl, Aryl, and Hydride Complexes of a Bulky Dipyrromethene Ligand. *Organometallics* **2014**, *33*, 4503−4511.

(11) Ballmann, G.; Elsen, H.; Harder, S. Magnesium Cyanide or Isocyanide? *Angew. Chem. Int. Ed.* **2019**, *58*, 15736−15741.

(12) Ballmann, G.; Rösch, B.; Harder, S. Stabilization of Heteroleptic Heavier Alkaline Earth Metal Complexes with an Encapsulating Dipyrromethene Ligand. *Eur. J. Inorg. Chem.* **2019**, *2019*, 3683−3689.

(13) Yu, C.; Zhang, P.; Gao, F.; Zhang, S.; Li, X. A Displacement-Type Fluorescent Probe Reveals Active Species in the Coordinative Polymerization of Olefins. *Polym. Chem.* **2018**, *9*, 603−610.

(14) Wan, W.; Silva, M. S.; McMillen, C. D.; Creager, S. E.; Smith, R. C. Highly Luminescent Heavier Main Group Analogues of Boron-Dipyrromethene. *J. Am. Chem. Soc.* **2019**, *141*, 8703−8707.

(15) King, E. R.; Hennessy, E. T.; Betley, T. A. Catalytic C-H Bond Amination from High-Spin Iron Imido Complexes. *J. Am. Chem. Soc.* **2011**, *133*, 4917−4923.

(16) Richter, T.; Thum, S.; Townrow, O. P. E.; Wiesinger, M.; Langer, J.; Harder, S. Synthesis, Structure, and Reactivity of a Superbulky Low-Valent β-diketiminate Ga(I) Complex. *Z. Anorg. Allg. Chem.* **2024**, No. e202400044.

(17) Hardman, N. J.; Power, P. P. Unique Structural Isomerism Involving Tetrazole and Amide/Azide Derivatives of Gallium. *Chem. Commun.* **2001**, *13*, 1184−1185.

(18) Stender, M.; Eichler, B. E.; Hardman, N. J.; Power, P. P.; Prust, J.; Noltemeyer, M.; Roesky, H. W. Synthesis and Characterization of $HC\{C(Me)N(C_6H_3\text{-}2,6\text{-}i\text{-}Pr_2)\}_2MX_2$ (M = Al, X = Cl, I; M = Ga, In, X = Me, Cl, I): Sterically Encumbered β-Diketiminate Group 13 Metal Derivatives. *Inorg. Chem.* **2001**, *40*, 2794−2799.

(19) Laubenstein, R.; Ahrens, M.; Braun, T. Synthesis and Structures of Gallium-β-Diketiminate Complexes: Isolation of a Dinuclear Gallium(II) Complex. *Z. Anorg. Allg. Chem.* **2017**, *643*, 1723−1729.

(20) Gyton, M. R.; Leverett, A. R.; Cole, M. L.; McKay, A. I. Bulky Bis(Aryl)Triazenides: Just Aspiring Amidinates? A Structural and Spectroscopic Study. *Dalton Trans.* **2020**, *49*, 5653−5661.

(21) Hardman, N. J.; Wright, R. J.; Phillips, A. D.; Power, P. P. Synthesis and Characterization of the Neutral "Digallene" Ar′GaGaAr′ and Its Reduction to $Na_2Ar'GaGaAr'$ (Ar′=2,6-$Dipp_2C_6H_3$, Dipp = 2,6-$iPr_2C_6H_3$). *Angew. Chem. Int. Ed.* **2002**, *41*, 2842−2844.

(22) Jones, C.; Junk, P. C.; Kloth, M.; Proctor, K. M.; Stasch, A. Bulky Amidinato Complexes and Amidine Adducts of Al, Ga and In Halides. *Polyhedron* **2006**, *25*, 1592−1600.

(23) Uhl, W.; El-Hamdan, A.; Prött, M.; Spuhler, P.; Frenking, G. $Ga_2I_2[C(SiMe_3)_3]_2$ - an Organogallium(II) Halide Containing a Ga-Ga Single Bond. *Dalton Trans.* **2003**, *7*, 1360−1364.

(24) Lee, V. Ya.; Fukawa, T.; Nakamoto, M.; Sekiguchi, A.; Tumanskii, B. L.; Karni, M.; Apeloig, Y. $(^tBu_2\ MeSi)_2Sn$ = $Sn(SiMe^tBu_2)_2$: A Distannene with a > Sn = Sn< Double Bond That Is Stable Both in the Solid State and in Solution. *J. Am. Chem. Soc.* **2006**, *128*, 11643−11651.

(25) Hawley, A. L.; Ohlin, C. A.; Fohlmeister, L.; Stasch, A. Heavier Group 13 Metal(I) Heterocycles Stabilized by Sterically Demanding Diiminophosphinates: A Structurally Characterized Monomer-Dimer Pair For Gallium. *Chem. Eur. J.* **2017**, *23*, 447−455.

(26) Driess, M.; Grützmacher, H. Main Group Element Analogues of Carbenes, Olefins, and Small Rings. *Angew. Chem. Int. Ed.* **1996**, *35*, 828−856.

(27) Barthélemy, A.; Scherer, H.; Weller, H.; Krossing, I. How long are Ga = Ga double bonds and Ga-Ga single bonds in dicationic gallium dimers? *Chem. Commun.* **2023**, *59*, 1353−1356.

(28) Hicks, J.; Juckel, M.; Paparo, A.; Dange, D.; Jones, C. Multigram Syntheses of Magnesium(I) Compounds Using Alkali Metal Halide Supported Alkali Metals as Dispersible Reducing Agents. *Organometallics* **2018**, *37*, 4810−4813.